

# Drug evaluation in cardiomyocytes derived from human induced pluripotent stem cells carrying a long QT syndrome type 2 mutation

Elena Matsa<sup>1</sup>, Divya Rajamohan<sup>1</sup>, Emily Dick<sup>1</sup>, Lorraine Young<sup>1</sup>, Ian Mellor<sup>2</sup>, Andrew Staniforth<sup>3</sup>, and Chris Denning<sup>1\*</sup>

<sup>1</sup>Wolfson Centre for Stem Cells, Tissue Engineering & Modelling, University of Nottingham, Nottingham NG7 2RD, UK; <sup>2</sup>School of Biology, University of Nottingham, Nottingham NG7 2RD, UK; and <sup>3</sup>Department of Cardiovascular Medicine, QMC, Nottingham NG7 2UH, UK

Received 4 February 2011; revised 15 February 2011; accepted 22 February 2011; online publish-ahead-of-print 2 March 2011

## Aims

Congenital long QT syndromes (LQTSs) are associated with prolonged ventricular repolarization and sudden cardiac death. Limitations to existing clinical therapeutic management strategies prompted us to develop a novel human *in vitro* drug-evaluation system for LQTS type 2 (LQT2) that will complement the existing *in vitro* and *in vivo* models.

## Methods and results

Skin fibroblasts from a patient with a *KCNH2* G1681A mutation (encodes  $I_{Kr}$  potassium ion channel) were reprogrammed to human induced pluripotent stem cells (hiPSCs), which were subsequently differentiated to functional cardiomyocytes. Relative to controls (including the patient's mother), multi-electrode array and patch-clamp electrophysiology of LQT2–hiPSC cardiomyocytes showed prolonged field/action potential duration. When LQT2–hiPSC cardiomyocytes were exposed to E4031 (an  $I_{Kr}$  blocker), arrhythmias developed and these presented as early after depolarizations (EADs) in the action potentials. In contrast to control cardiomyocytes, LQT2–hiPSC cardiomyocytes also developed EADs when challenged with the clinically used stressor, isoprenaline. This effect was reversed by  $\beta$ -blockers, propranolol, and nadolol, the latter being used for the patient's therapy. Treatment of cardiomyocytes with experimental potassium channel enhancers, nicorandil and PD118057, caused action potential shortening and in some cases could abolish EADs. Notably, combined treatment with isoprenaline (enhancers/isoprenaline) caused EADs, but this effect was reversed by nadolol.

## Conclusions

Findings from this paper demonstrate that patient LQT2–hiPSC cardiomyocytes respond appropriately to clinically relevant pharmacology and will be a valuable human *in vitro* model for testing experimental drug combinations.

## Keywords

Human induced pluripotent stem cells • Cardiomyocytes • Long QT syndrome • Electrophysiology • Pharmacological response • Arrhythmias • Early after depolarizations

## Introduction

The hereditary long QT syndromes (LQTSs) are characterized by abnormal ventricular repolarization and are a recognized cause of sudden cardiac death (SCD) syndrome.<sup>1</sup> Patients with LQTS carry an increased risk of *Torsades de Pointes* [polymorphic ventricular

tachycardia (PMVT)], which can present with a host of clinical manifestations varying from palpitations, syncope (fainting), and seizures<sup>2,3</sup> to cardiac arrest and sudden death.<sup>4</sup> Long QT syndrome has been associated with over 500 different mutations in at least 13 genes encoding cardiac ion channel proteins.<sup>5</sup> The estimated genotype-to-phenotype correlation of 60–75% depends on

\* Corresponding author. Tel: +44 115 82 31236, Fax: +44 115 82 31230, Email: [chris.denning@nottingham.ac.uk](mailto:chris.denning@nottingham.ac.uk)

Published on behalf of the European Society of Cardiology. All rights reserved. © The Author 2011. For permissions please email: [journals.permissions@oup.com](mailto:journals.permissions@oup.com).

The online version of this article has been published under an open access model. Users are entitled to use, reproduce, disseminate, or display the open access version of this article for non-commercial purposes provided that the original authorship is properly and fully attributed; the Journal, Learned Society and Oxford University Press are attributed as the original place of publication with correct citation details given; if an article is subsequently reproduced or disseminated not in its entirety but only in part or as a derivative work this must be clearly indicated. For commercial re-use, please contact [journals.permissions@oup.com](mailto:journals.permissions@oup.com).

the location of the mutation on the ion channel.<sup>6</sup> In general, mutations in the pore-forming regions have been linked to more severe phenotypes, but large variations in penetrance are seen even among family members carrying the same mutation.<sup>7</sup> The incidence of LQTS is estimated to be 1:1000 individuals, 45% of whom are diagnosed with LQTS type 2 (LQT2). LQT2 is caused by mutations in the *KCNH2* (also known as human Ether-a-go-go Related Gene; *HERG*) gene, which forms the  $\alpha$ -subunit of the rapid-acting inward rectifying potassium ( $I_{kr}$ ) channel.<sup>8</sup> Such mutations have a dominant negative effect leading to reduced  $I_{kr}$  function, which arises due to inappropriate protein maturation, impaired protein trafficking, or altered gating properties induced in the wild-type channel.<sup>9</sup>

Current treatments for LQT2 include the use of  $\beta$ -adrenoreceptor antagonists ( $\beta$ -blockers), especially nadolol, a non-selective class II anti-arrhythmic agent.<sup>10</sup> Even though  $\beta$ -blockers are able to reduce the risk of cardiac episodes by 59%, 23% of LQT2 patients still experience cardiac episodes.<sup>11</sup> In these cases, and in patients otherwise felt to be at high risk of a cardiac event,<sup>12</sup> surgery is required for implantation of a cardioverter defibrillator (ICD). Left cardiac sympathetic denervation<sup>13,14</sup> may also be of value in patients where surges in sympathetic nerve activity are causal in arrhythmogenesis. However, these invasive procedures carry a risk of infection, can be traumatic to patients, and are technically more demanding and liable to complication in small children and infants. *In vitro* transgenic<sup>15,16</sup> and animal models, such as cultured guinea-pig myocytes or arterially perfused canine and rabbit left ventricular wedge preparations,<sup>6</sup> as well as *in vivo* toxicity studies in monkeys or dogs have been used to develop and safety screen novel pharmacological treatments for LQTS. However, these models are not always predictive of drug activity in human patients<sup>8,10</sup> and additional humanized test platforms would be beneficial.

Induced pluripotency involves reprogramming of somatic cells into human induced pluripotent stem cells (hiPSCs) by introducing genetic factors such as *OCT4*, *SOX2*, *NANOG*, and *LIN28*.<sup>17</sup> The produced hiPSCs can be differentiated into a wide range of cell types, including functional cardiomyocytes, and this has opened new avenues for the generation of humanized *in vitro* models of disease. A key goal is to produce a model of LQTS that responds appropriately to clinically relevant pharmacology. This could provide an opportunity to identify new routes of pharmacological intervention and better tools to improve risk stratification management. Direct comparison of a particular patient genotype with phenotype or drug response may also be possible. Therefore, to explore these notions further, we generated patient-specific hiPSCs from an individual suffering from LQT2 due to a *KCNH2* mutation in the pore-forming region of  $I_{kr}$ . In addition, hiPSCs were produced from the patient's mother, who carries the same mutation but is clinically asymptomatic for cardiac episodes. Cardiomyocytes were derived from these hiPSCs, and from genetically unrelated human pluripotent stem cells that did not carry the mutation. Myocytes were analysed by electrophysiology, with responses to existing and novel therapeutic drugs being examined. The data presented for potassium channel and  $\beta$ -adrenoreceptor modulators show the potential utility of patient-specific hiPSC-derived cardiomyocytes in drug evaluation.

## Methods

For details on hiPSCs, including generation, culture, differentiation, and characterization, see Supplementary material online (Supplementary Methods), and Dick *et al.*<sup>18</sup> and Anderson *et al.*<sup>19</sup>

### Mutation analysis of genomic DNA

To confirm the presence of the *KCNH2* G1681A mutation in patient-specific fibroblasts and derived hiPSCs, genomic DNA was extracted from frozen cell pellets (QIAGEN DNeasy Blood and Tissue kit). Polymerase chain reaction (PCR) was performed using 25  $\mu$ L reaction mixture, which comprised Hotstar Taq polymerase (0.125  $\mu$ L; QIAGEN), 5  $\mu$ M forward and reverse primers (F: GGAAGCTG GATCGCTACTCA, R: GAAGTAGAGCGCCGTACAT, 2.5  $\mu$ L; Invitrogen), 10 $\times$  buffer (2.5  $\mu$ L; QIAGEN), 2.5 mM dNTPs (2.5  $\mu$ L; Invitrogen) and 1  $\mu$ L of genomic DNA diluted to 100 ng/ $\mu$ L. The PCR conditions were 95°C for 15 min, then 35 cycles (95°C, 1 min; 55°C, 30 s; 72°C, 1 min) and a final extension step at 72°C for 5 min. Polymerase chain reaction products were electrophoresed on a 1.5% agarose gel, purified (QIAGEN QIAquick Gel Extraction kit), and sequenced using the reverse primer.

### Analysis of *KCNH2* 1681 allele-specific expression

RNA extraction from cells performed using the RNeasy Mini kit (QIAGEN). Reverse transcription was performed using the First Strand cDNA Synthesis kit (GE Healthcare), with 100 ng RNA. Reverse transcription-PCR was performed as above, with 2  $\mu$ L of cDNA, and addition of 2.5 mM MgCl<sub>2</sub> (1  $\mu$ L; QIAGEN) for detection of the mutant allele. Primers used for the wild-type allele were F: ACTTCAAGGGCTGGTTCCTC and R: ATGCAGGCTAGCCAG TGCTC, and for the mutant allele were F: CTCTGGCTCTGAGGA GCTGA and R: ATGCAGGCTAGCCAGTGCTT. Polymerase chain reaction conditions were 95°C for 15 min, then 37 cycles (95°C, 1 min; 55°C, 30 s; 72°C, 1 min) with final extension at 72°C for 5 min.

### Statistical analysis

Statistical analysis was performed using NCSS software for Windows v7.1.15. The Kruskal-Wallis *H* test was used for analysis of non-parametric independent data groups, and pair-wise comparisons were performed using the Mann-Whitney's *U* test. Tests were two-tailed and significance was assessed at a level of 0.05. Within-group data are reported as mean values of experimental replicates  $\pm$  the standard deviation of the mean to increase sensitivity towards biological replicate experiments.

## Results

### Patient history and genetic profile

The female LQT2 patient in this study presented at age of 15 years with 11 episodes of syncope in 12 months with seizure on occasions. She was a competitive swimmer, but had never experienced episodes in relation to this activity. Episodes were nocturnal and, whilst ECG monitored on the ward, were typically seen to occur with arousal from sleep. This was indicative of LQT2, since auditory stimuli causing arousal from sleep are described as precipitants for ventricular arrhythmia in *KCNH2* mutations.<sup>3</sup> A clinical episode of PMVT at rates of 230 bpm is shown in Figure 1A, with full 12-lead ECGs in Supplementary material

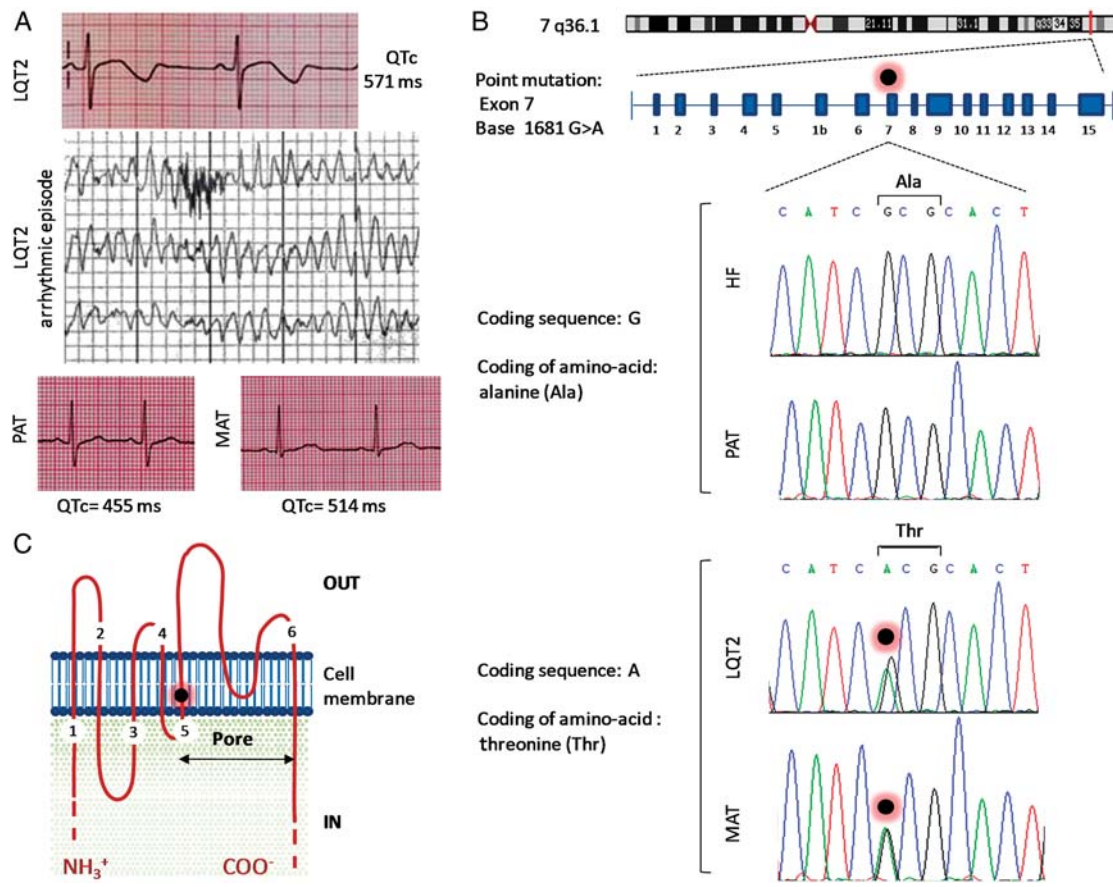


**Figure 1** Clinical and genetic profile of the LQT2 family. (A) Electrocardiogram of the LQT2 patient, showing prolonged QTc interval of up to 571 ms (lead V5) and arrhythmic episode recorded during telemetry. Electrocardiograms of patient's father (PAT; lead V5) and mother (MAT; lead V5) are also presented. (B) Schematic diagram showing location of the *KCNH2* gene on chromosome 7q36.1 and position of autosomal dominant point mutation in exon 7, at base 1681 of the coding sequence (G1681A). This missense mutation results in substitution of the hydrophobic amino acid alanine (Ala), at position 561 of the protein, by the hydrophilic amino acid threonine (Thr; p.Ala561Thr). Results of genomic DNA sequencing in fibroblasts derived from hESCs (HF) and blood samples taken in hospital from LQT2 patient, mother, and father. (C) Schematic representation of the  $I_{kr}$  potassium channel showing that *KCNH2* p.Ala561Thr mutation is located in the S5 transmembrane domain (black dot with red halo), which is involved in the pore-forming region of the channel.

online, Figure S1. The patient never experienced cardiac arrest or needed cardiac resuscitation, and there was no family history of sudden adult death syndrome. Whereas the patient's echocardiogram, MRI, and signal-averaged electrocardiography were normal, her QTc interval was up to 571 ms (Figure 1A; Supplementary material online, Figure S1). Genetic screening showed that she carried an LQT2-associated autosomal dominant point mutation at *KCNH2* (G1681A; Figure 1B). The mutation causes an alanine to threonine substitution at position 561 of the encoded protein (p.Ala561Thr) and is located in the pore-forming region of the  $I_{kr}$  channel, at transmembrane segment S5 (Figure 1C),<sup>20</sup> and prevents post-translational maturation of *KCNH2*.<sup>21</sup> With a QTc >500 ms, a documented LQT2 gene mutation, and an adverse clinical history, the patient was felt to be at significant risk of a future arrhythmic event and received a primary prevention ICD.<sup>12</sup> She has so far remained arrhythmia free for 4 years on  $\beta$ -blocker (nadolol) treatment. The patient's mother (55 years) is an asymptomatic carrier of the same mutation and is not

currently under treatment but does have a prolonged QTc of up to 514 ms (Figure 1A and B). The father does not carry the mutation and has a QTc of 445 ms (Figure 1A and B).

### Derivation and characterization of hiPSC lines

Human iPSCs were produced by reprogramming primary skin fibroblasts isolated from 4 mm punch biopsies taken from the LQT2 patient (LQT2-hiPSC) and mother (MAT-hiPSC) (Figure 2; Supplementary material online, Figure S2). HF-hiPSC were produced from genetically unrelated hESC-derived fibroblasts (Supplementary material online, Figure S2), while HUES7 cells were used as a hESC control.<sup>22</sup> Generation of hiPSCs was by lentiviral delivery of human *OCT4*, *SOX2*, *NANOG*, and *LIN28* (Figure 2; Supplementary material online, Figure S2).<sup>18</sup>

Sequencing of genomic DNA showed that the G1681A mutation in *KCNH2* was present in LQT2-hiPSCs and MAT-

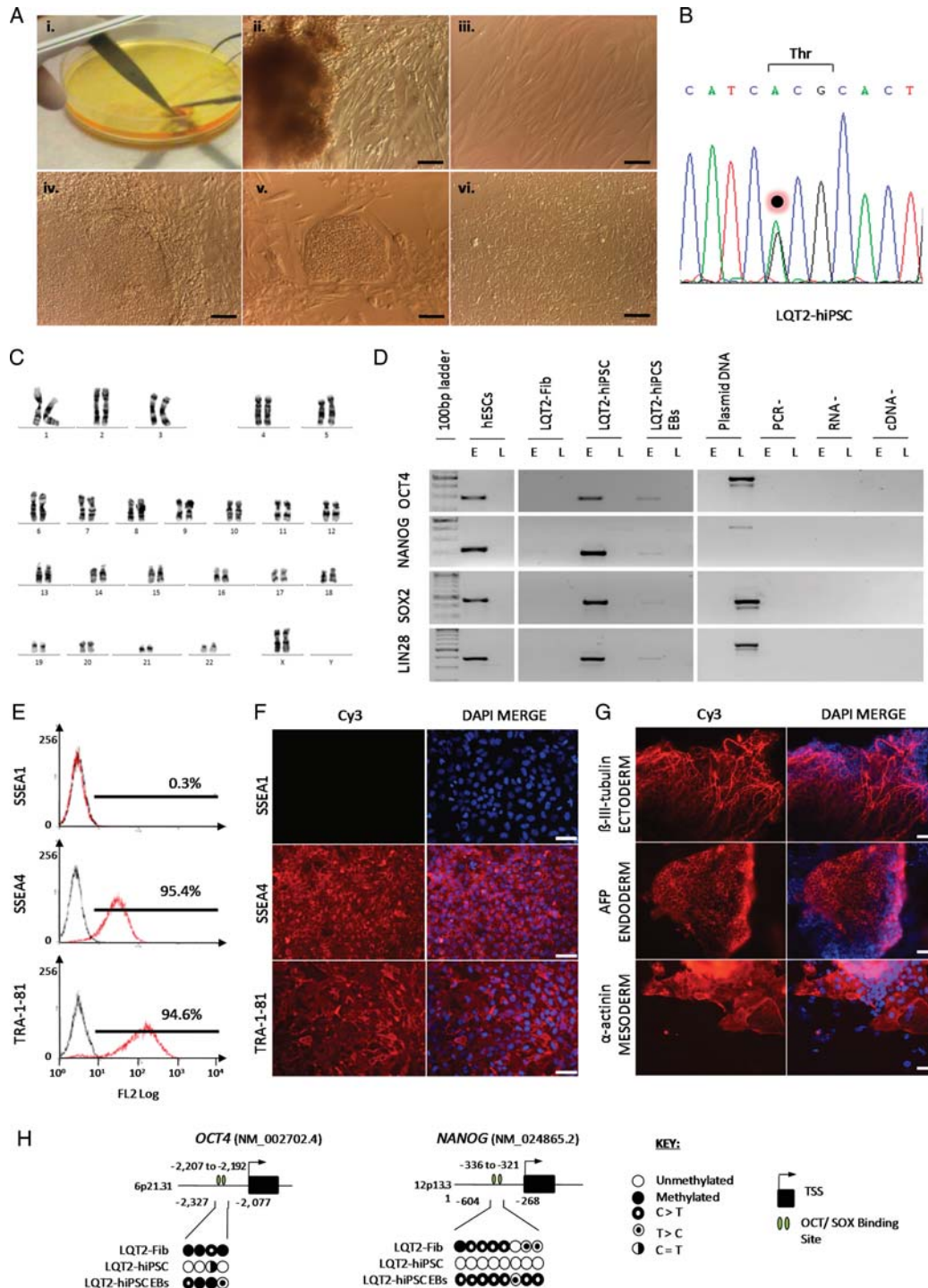


**Figure 2** Derivation and characterization of LQT2 fibroblasts and hiPSCs. (A) (i) Processing a 4 mm skin biopsy isolated from the LQT2 patient. (ii) Fibroblast outgrowths from digested skin sample, (iii) monolayer culture of LQT2 fibroblasts (LQT2-Fib), (iv) hiPSC colony generated from LQT2-Fib following lentiviral transduction with *OCT4*, *NANOG*, *SOX2*, and *LIN28*, (v) LQT2-hiPSC colony at passage 1, (vi) monolayer culture of LQT2-hiPSCs at passage 15, grown in feeder-free conditions on Matrigel. Scale bars represent 100  $\mu$ m. (B) Genomic sequencing in LQT2-hiPSCs showing maintenance of the *KCNH2* G1681A mutation. (C) Karyogram of LQT2-hiPSCs showing a normal 46XX karyotype, at passage 15. (D) RT-PCR analysis of *OCT4*, *NANOG*, *SOX2*, and *LIN28* expression from endogenous (E) and lentiviral (L) loci in LQT2-Fib, LQT2-hiPSCs, LQT2-hiPSC embryoid bodies. (E) Flow cytometry and (F) immunostaining for differentiation marker, SSEA1, and pluripotency markers, TRA-1-81 and SSEA4, in LQT2-hiPSCs. (G) Immunostaining in LQT2-hiPSC embryoid bodies for the germ layer markers  $\beta$ -III-tubulin (ectoderm),  $\alpha$ -fetoprotein (AFP; endoderm), and  $\alpha$ -actinin (mesoderm). Scale bars in (E) and (F) represent 65  $\mu$ m. (H) DNA methylation analysis for *OCT4* and *NANOG* in LQT2-Fib, LQT2-hiPSC, and LQT2-hiPSC embryoid bodies, showing hypomethylation of hiPSCs relative to Fib and embryoid body samples.

hiPSC, but not in HF-hiPSC (Figure 2; Supplementary material online, Figure S2), and HUES7 hESCs were confirmed as normal. Correspondingly, allele-specific RT-PCR showed mutant *KCNH2* G1681A transcripts were present in cells differentiated from LQT2-hiPSCs and MAT-hiPSC, but not from HF-hiPSC or HUES7 (see Supplementary material online, Figure S2). Thus, mutation analysis *in vitro* was consistent with the patient data.

All hiPSC lines had a normal karyotype (Figure 2) and displayed population doubling rates similar to hESCs (see Supplementary material online, Figure S2).<sup>23</sup> Flow cytometry and immunostaining showed that hiPSCs had silenced the fibroblast-specific marker P4HB and the differentiation marker SSEA1, and had reactivated the pluripotency markers TRA-1-81, SSEA4, OCT4, NANOG, SOX2, LIN28, DNMT3B, REX1, KLF4, and cMYC (Figure 2; Supplementary material online, Figure S3). Reverse transcription PCR analysis confirmed that the reprogramming factors *OCT4*, *NANOG*, *SOX2*, and *LIN28* were reactivated in the endogenous loci, while lentiviral transgenes were silenced (Figure 2; Supplementary material online, Figure S2). Regulatory regions within the *OCT4* and *NANOG* promoters acquired a hypomethylated state in hiPSCs, relative to the originating fibroblasts and hiPSC differentiated progeny (Figure 2). EB differentiation from hiPSCs showed contribution to the three embryonic germ layers; endoderm, ectoderm, and mesoderm via expression of the markers  $\beta$ -III-tubulin,  $\alpha$ -fetoprotein, and cardiac  $\alpha$ -actinin (Figures 2 and 3A). This confirmed that hiPSC lines were pluripotent.

## Derivation and characterization of cardiomyocytes

Differentiation of hiPSC lines to cardiomyocytes was induced via embryoid bodies (EBs).<sup>22</sup> Spontaneously beating clusters appeared from d11 of differentiation and occurred at similar efficiencies between the lines (not shown). Between d25–30, beating clusters were mounted onto multi-electrode arrays (MEAs) for electrophysiology analysis (Figure 3B and D). Alternatively, they were dissociated into single cardiomyocytes, which provided single cells for patch clamp analysis (Figure 3C) and immunofluorescence staining (Figure 3A). Cardiomyocytes from patient and control lines expressed the cardiac markers,  $\alpha$ -actinin and Troponin-I, and showed characteristic cardiac muscle striations (Figure 3A).

Patch clamp analysis of single cardiomyocytes demonstrated formation of ventricular, atrial, and pacemaker subtypes, as determined by the morphology of action potentials generated (Figure 3C)<sup>24</sup> and by the ratio of APD90/APD50 (Figure 3E). This allowed comparison of action potential duration (APD) for different cardiomyocyte subtypes derived from the hiPSC lines. Action potential duration of ventricular and atrial myocytes from LQT2-hiPSC was prolonged ( $881 \pm 204.8$  and  $870.2 \pm 165.3$  ms, respectively) relative to those from HF-hiPSC ( $386.2 \pm 138.7$  and  $467.1 \pm 75.8$  ms) and hESCs ( $419.1 \pm 123.8$  and  $642 \pm 35.5$  ms) (Figure 4). However, MAT-hiPSC ventricular and atrial cardiomyocytes had APDs of  $704.45 \pm 57$  ms and  $667.6 \pm 156.0$ , which were shorter than the values for the LQT2-hiPSC but longer than for HF-hiPSC and hESC myocytes (Figure 4). Action

potential duration measured at 50 and 90% repolarization showed similar prolongation in ventricular LQT2-hiPSC myocytes (Figure 4). Pacemaker myocytes did not show significant differences between the lines (Figure 4).

To determine whether similar data could be extracted from beating clusters, we used MEA analysis. This showed that the field potential duration (FPD) of LQT2-hiPSC myocytes was significantly prolonged ( $1026.5 \pm 203.6$  ms;  $P = 0.007$ ; Figure 3B) relative to those from MAT-hiPSC ( $658.3 \pm 115.9$  ms) or controls (HF-hiPSC,  $644.3 \pm 133.4$  ms; hESC,  $859.5 \pm 75.5$  ms).

Together, these data are in agreement with the long QTc intervals seen in the clinical ECG data. However, they suggest that patch clamp analysis of APDs is more sensitive because prolonged durations were detected in myocytes from LQT2-hiPSC and MAT-hiPSC, whereas MEA analysis detected FPD prolongation only in LQT2-hiPSC myocytes.

## Sensitivity of LQT2 cardiac myocytes to $\beta$ -adrenoreceptor agonists and antagonists

Specific genotype-phenotype correlations for triggers of life-threatening events have been reported between the LQT syndromes. Stimulation of the sympathetic nervous system appears to be generally important; for LQT2 13 and 43% of episodes occur with exercise and strong emotion, respectively. Auditory stimuli have been linked to 26% of episodes in LQT2 patients.<sup>25</sup> Indeed, stress testing of patients via sympathetic stimulation by the  $\beta$ -adrenoreceptor agonist, isoprenaline, has been employed to exacerbate and diagnose LQTS.<sup>26</sup> To determine whether arrhythmic events could be recapitulated *in vitro*, patient-specific and control cardiomyocytes were treated with isoprenaline (Figure 5). In beating clusters, isoprenaline caused a similar reduction in FPD of control ( $20.4 \pm 11.8\%$ ; data pooled for MAT-hiPSC, HF-hiPSC, and HUES7) and LQT2-hiPSC ( $24.1 \pm 12.7\%$ ;  $P > 0.05$ ; Figure 5A). However, LQT2-hiPSC myocytes dissociated to single cells were more sensitive to isoprenaline treatment and showed a significantly larger reduction ( $35.8 \pm 15.2\%$ ;  $P = 0.018$ ) in APD relative to control cells ( $10.5 \pm 6.7\%$ ; Figure 5B). APD50 and APD90 values were affected similarly (Figure 5B and C). Subsequent treatment with  $\beta$ -adrenoreceptor antagonists (or  $\beta$ -blockers), nadolol and propranolol, resulted in a  $30 \pm 19\%$  increase in APD, in both LQT2-hiPSC and control myocytes, and had a more pronounced effect on APD50 than APD90 (Figure 5C).

In 25% of dissociated LQT2-hiPSC myocytes, treatment with isoprenaline resulted in the appearance of electrophysiological abnormalities, including early after depolarizations (EADs; Figure 5D and E). In some cases,  $>50$  consecutive beats were followed by EADs. Such events were never observed in control myocytes. Isoprenaline-induced arrhythmias in LQT2-hiPSC myocytes were ameliorated by nadolol or propranolol. These *in vitro* results are consistent with clinical observations, where  $\beta$ -blockers are used to regulate cardiac episodes in LQT2 patients. Specifically, nadolol is currently the treatment of choice for the LQT2 patient in this study, and propranolol has been shown to suppress the influence of sympathetic stimulation in LQT2 patients.<sup>10,11,27</sup>

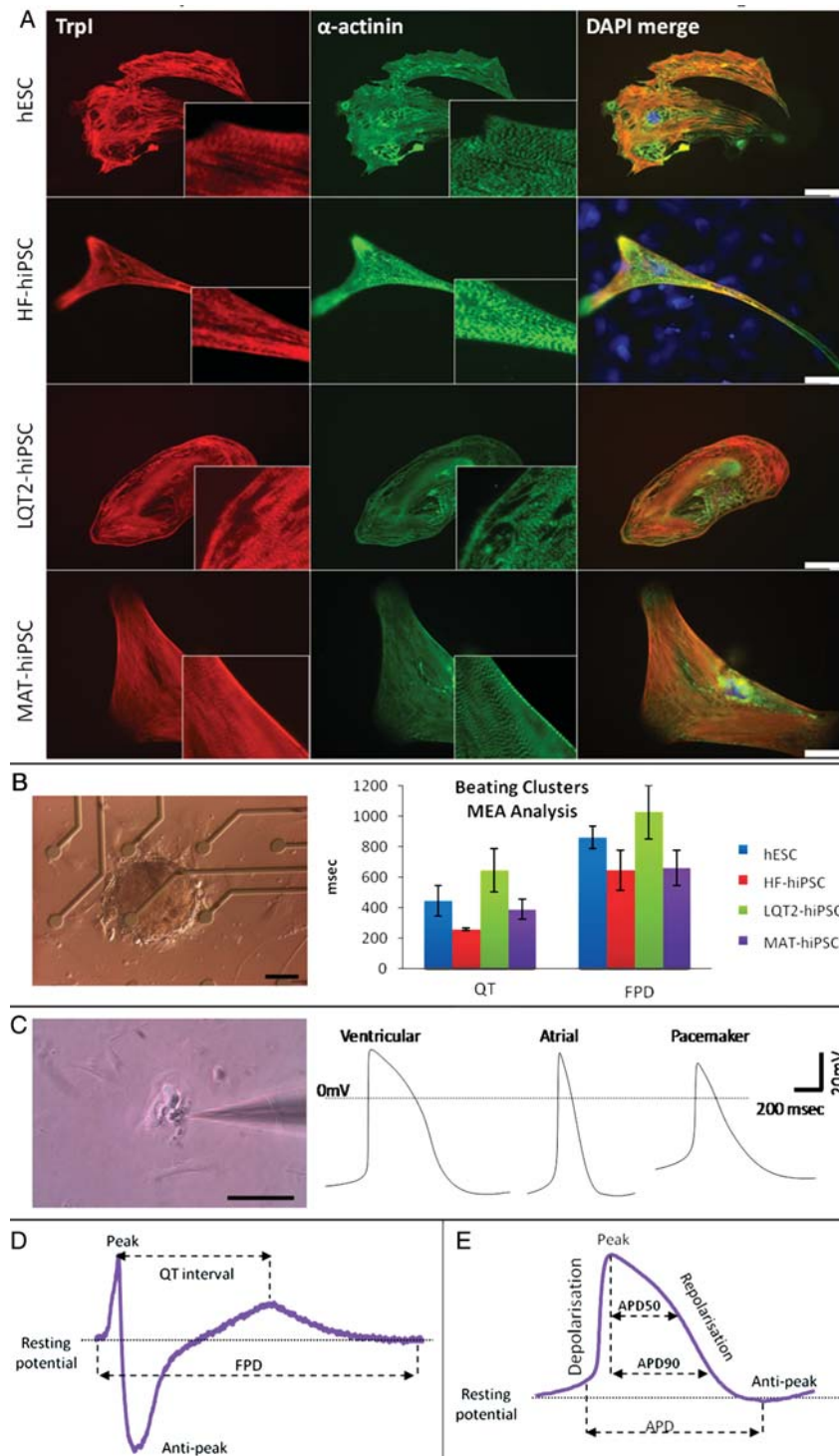
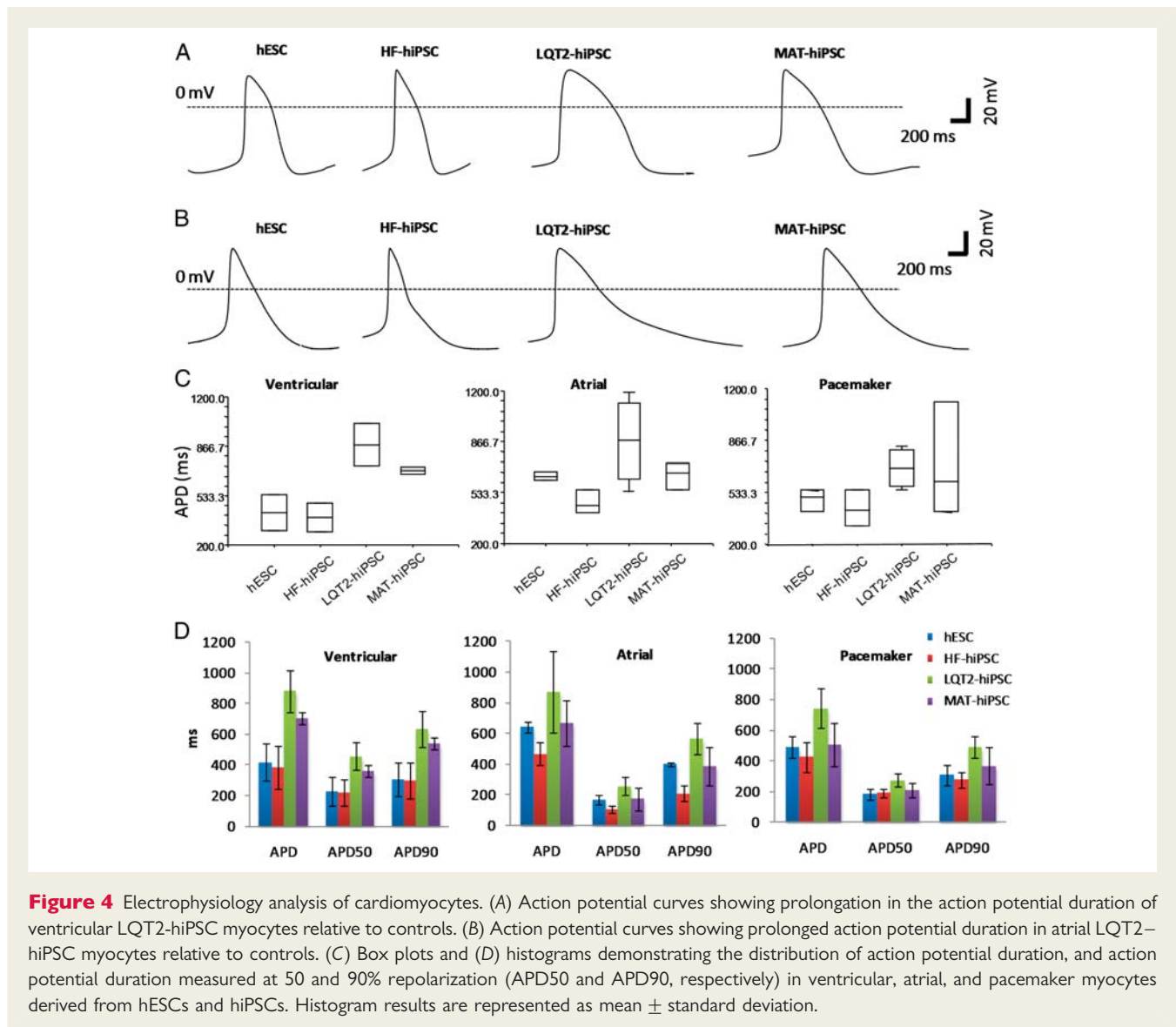


**Figure 3** Characterization of cardiac myocytes. (A) Immunostaining for cardiac troponin I (TrpI) and  $\alpha$ -actinin in myocytes derived from hESCs, HF-hiPSC, LQT2-hiPSC, and MAT-hiPSC, showing characteristic cardiac muscle striations. (B) Image of an LQT2-hiPSC beating cluster mounted onto a multi-electrode array for electrophysiology analysis, and graph showing prolongation in QT interval and field potential duration in LQT2-hiPSC beaters relative to controls. (C) Image of a single LQT2-hiPSC beating cell undergoing patch-clamp analysis, and action potential curves representing formation of ventricular, atrial, and pacemaker myocytes. (D) Schematic diagram of a multi-electrode array trace, showing how results were analysed to calculate duration of the QT interval and field potential duration. (E) Schematic diagram of a patch-clamp trace, showing how results were analysed to calculate duration of the action potential and the action potential duration at 50 and 90% repolarization (APD50 and APD90, respectively). To determine the type of cardiac myocyte analysed, APD90/50 values < 1.4 designated ventricular cells, 1.4–1.7 designated pacemaker cells, and > 1.7 designated atrial cells. Scale bars represent 130  $\mu$ m.



## Response of LQT2 cardiac myocytes to potassium channel blockers and openers

To further characterize the response of LQT2-hiPSC myocytes to pharmacology, cells were treated with E4031 (Figure 6). This drug causes blockade of the  $I_{kr}$  current through binding to the inner cavity of the HERG channel in S6 or C-terminal domains.<sup>28</sup> In beating cells from all hiPSC sources, E4031 caused prolongation of FPD/APD (Figure 6A and B). This effect was particularly evident in phases 2 and 3 of the action potential (Figure 6B) and corresponds with the time when  $I_{kr}$  channels are most active.<sup>29</sup> E4031 treatment caused a 77.2% prolongation in the APD of LQT2-hiPSC myocytes and 51.5% in control myocytes. Most notably, E4031 treatment resulted in EADs in 30% of the LQT2-hiPSC myocytes (Figure 6C), but this response was never seen in controls.

The effect of two experimental potassium channel enhancers on cardiomyocyte FPD/APD was evaluated (Figure 6D and E); nicorandil, an  $I_{k_{ATP}}$  channel opener,<sup>30</sup> and PD-118057, a type 2  $I_{kr}$  channel

enhancer that attenuates channel closing.<sup>28</sup> In LQT2-hiPSC myocytes, the APD was shortened by 18.6% with nicorandil and was sufficient to abolish spontaneously occurring EADs (Figure 6G). Action potential duration was shortened by a further 29.5% (to 58.1%) with combined nicorandil and PD-118057 treatment (Figure 6E). Treatment with PD-118057 alone abbreviated the APD by 17.3% (Figure 6F). Both drugs exerted their effects in phases 2 and 3 of the action potential, consistent with their mechanism of action (Figure 6E and F). This shows potassium channel activators can normalize the prolonged repolarization of myocytes carrying a mutation in the KCNH2 pore-forming region.

Next we evaluated whether potassium channel enhancers could reverse the effect of the potassium channel blocker, E4031. Combined treatment with E4031/nicorandil elicited 21.9 and 10.1% APD shortening in control and LQT2-hiPSC myocytes (not shown). Triple treatment with E4031, nicorandil, and PD-118057 resulted in further shortening of the APD by 8.9 and 2.4% in control and LQT2-hiPSC myocytes (not shown). These data suggest that the severe effect of potassium channel blockers

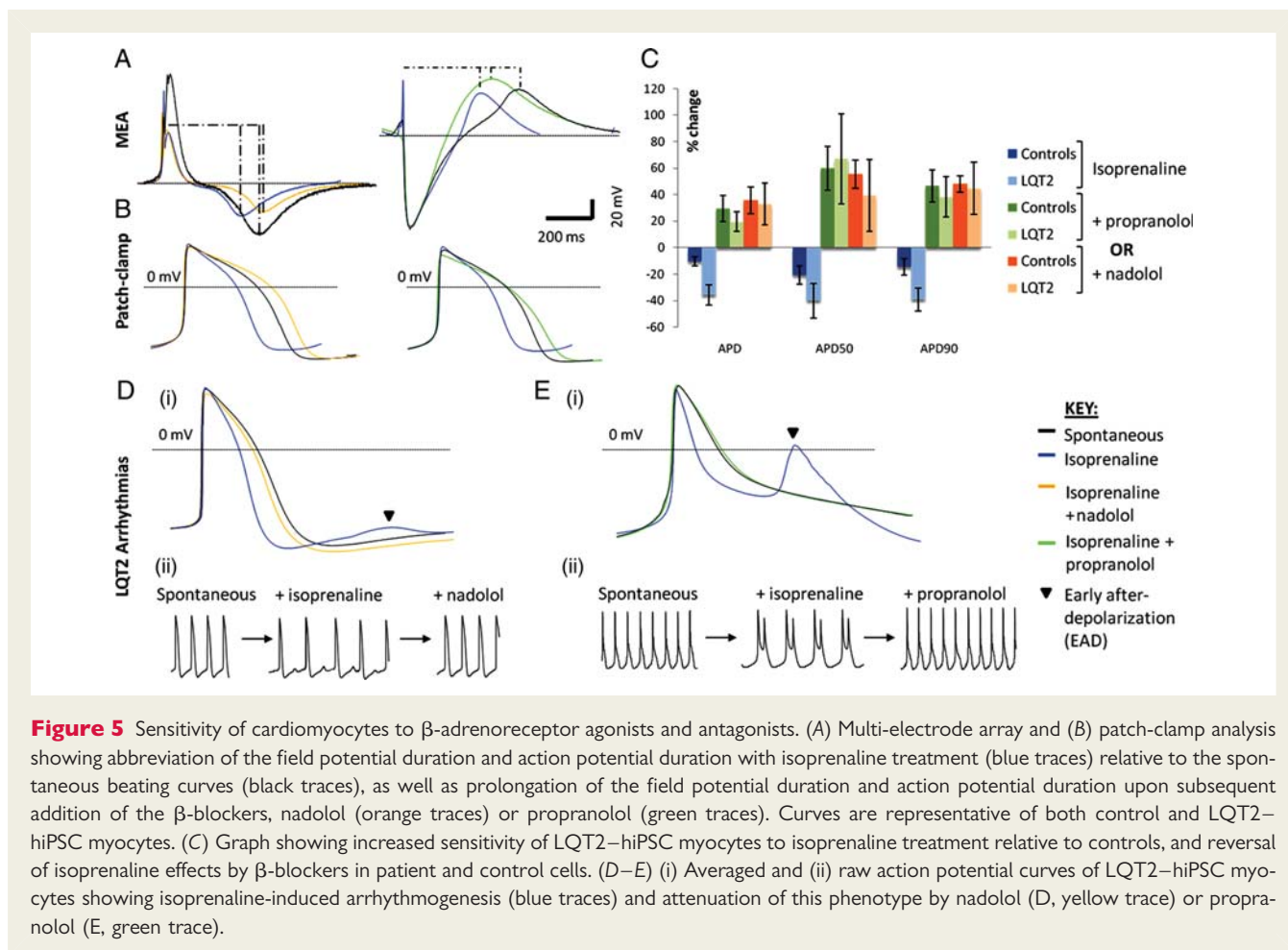


**Figure 5** Sensitivity of cardiomyocytes to  $\beta$ -adrenoreceptor agonists and antagonists. (A) Multi-electrode array and (B) patch-clamp analysis showing abbreviation of the field potential duration and action potential duration with isoprenaline treatment (blue traces) relative to the spontaneous beating curves (black traces), as well as prolongation of the field potential duration and action potential duration upon subsequent addition of the  $\beta$ -blockers, nadolol (orange traces) or propranolol (green traces). Curves are representative of both control and LQT2–hiPSC myocytes. (C) Graph showing increased sensitivity of LQT2–hiPSC myocytes to isoprenaline treatment relative to controls, and reversal of isoprenaline effects by  $\beta$ -blockers in patient and control cells. (D–E) (i) Averaged and (ii) raw action potential curves of LQT2–hiPSC myocytes showing isoprenaline-induced arrhythmogenesis (blue traces) and attenuation of this phenotype by nadolol (D, yellow trace) or propranolol (E, green trace).

seen in LQT2–hiPSC cardiomyocytes are challenging to reverse by potassium channel enhancers.

Finally, we evaluated the effect of the potassium channel enhancers on myocytes in which  $\beta$ -adrenoreceptor pathways had been stimulated or inhibited. As before, isoprenaline led to shortened APD (Figures 5 and 6H). Irrespective of the source of hiPSCs, myocytes treated with isoprenaline in combination with nicorandil and PD-118057 developed EADs (Figure 6H). These effects could be reversed by  $\beta$ -adrenoreceptor blockade with nadolol or propranolol (Figure 6H). This observation suggests that patients treated with potassium channel activators might run a higher risk of cardiac arrhythmogenesis, for example, during exercise when  $\beta$ -adrenoreceptor activation occurs.

## Discussion

We isolated skin fibroblasts from a patient carrying the autosomal-dominant missense mutation *KCNH2* G1681A, known to be associated with LQTS type 2. The patient fibroblasts were reprogrammed to hiPSCs, which were differentiated to spontaneously beating cardiomyocytes. The patient myocytes exhibited expression of cardiac markers and electrophysiological properties that confirmed their functionality, as previously shown in hESC- and hiPSC-derived cardiomyocytes.<sup>31</sup> Nevertheless, disease-

specific properties emerged in the LQT2–hiPSC myocytes, including prolongation of the FPD/APD in beating clusters as well as in atrial and ventricular cells, and increased sensitivity (appearance of EADs) to stress induced by  $\beta$ -adrenoreceptor agonists. Notably, although APD increases occurred in myocytes derived from MAT–hiPSC,  $\beta$ -adrenoreceptor stimulation did not lead to EADs. This is consistent with clinical data, which show that the mother is an asymptomatic carrier of the *KCNH2* G1681A mutation who presents with a prolonged QTc but does not require therapeutic intervention. This also supports the finding that large variations in phenotype can occur in family members carrying the same mutation.<sup>7,10</sup> Why this happens remains unexplained, but may relate to additional polymorphisms throughout the genome. Mutations in *KCNQ1* or *SCN5A*, which underlie LQT1 and LQT3, were not reported for the individuals in this study and further analysis is needed to identify genetic and biochemical differences between them. Clinically relevant  $\beta$ -blockers restored the action potential of LQT2–hiPSC myocytes to normal.<sup>11</sup> This included nadolol, which is the therapy used to regulate cardiac episodes in the LQT2 patient. Our findings also lend support to the responses seen in hiPSC-derived LQT1 *in vitro* cardiomyocyte models to  $\beta$ -adrenoreceptor agonists and antagonists.<sup>32</sup> Our data also demonstrated that potassium channel enhancers, such as nicorandil, are able to abolish EADs.



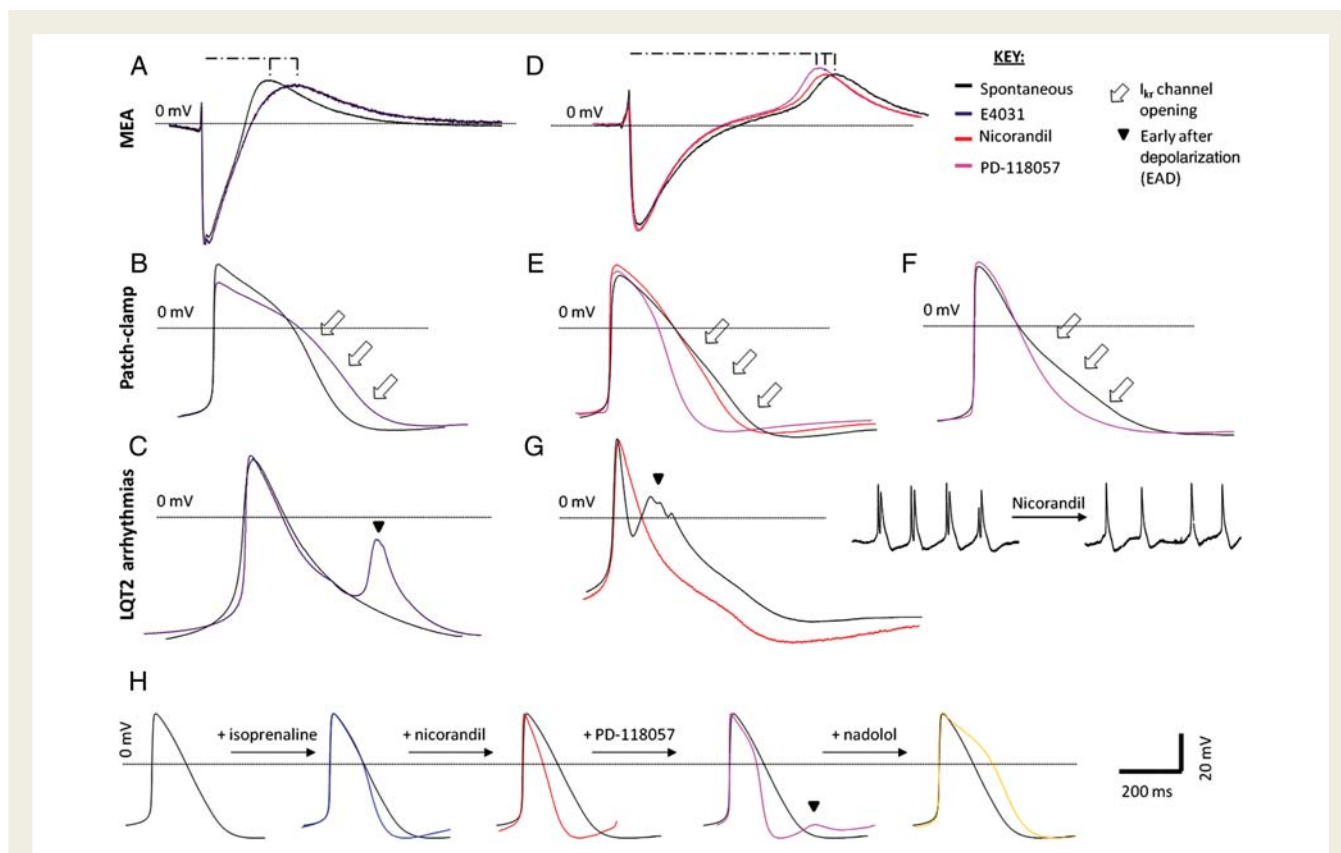


**Figure 6** Sensitivity of cardiomyocytes to potassium channel blockers and openers. (A) Multi-electrode array and (B) patch-clamp analysis showing elongation of the field potential duration and action potential duration with E4031 treatment (purple traces) relative to the spontaneous beating curves (black traces). Curves are representative of both control and LQT2–hiPSC myocytes. (C) Action potential curves of LQT2–hiPSC myocytes showing E4031-induced arrhythmogenesis. (D) Multi-electrode array and (E and F) patch-clamp analysis showing shortening of the field potential and action potential durations with nicorandil (red traces) and PD-118057 (pink traces) treatment. (G) Action potential curves showing spontaneously occurring early after depolarizations (black trace) abolished by nicorandil treatment (red trace). (H) Action potential traces of sequential drug treatment with isoprenaline, nadolol and PD-118057, resulting in the generation of early after depolarizations due to excessive action potential duration shortening (pink trace). The phenotype was then attenuated with nadolol treatment (yellow trace). (D–F) Curves of both control and LQT2–hiPSC myocytes.

Long QT syndrome type 2–hiPSC myocytes were more sensitive to treatment with the  $I_{kr}$  channel blocker, E4031. This suggests that LQT2 patients could be more susceptible to arrhythmogenesis by drugs that are known to inhibit the  $I_{kr}$  current and hence have the potential to prolong the QT interval, such as the recently withdrawn cisapride, terfenadine, and lidoflazine.<sup>33</sup> Arrhythmic events were not observed in control myocytes, but have previously been reported in hESC-derived cardiomyocytes treated with high doses of E4031.<sup>34</sup> Treatment with the experimental potassium channel enhancers, nicorandil and PD-118057, subsequent to E4031, had only a moderate effect on abbreviating the APD. In the case of the  $I_{k_{ATP}}$  activator, nicorandil, this was likely due to administration of low drug doses, since high (10–20  $\mu$ M) doses have previously been shown to reverse HERG blockade in LQT2 canine models.<sup>35</sup> For PD-118057, the moderate effect was likely due to differences in  $I_{kr}$  channel-binding sites and a different mechanism of action when compared with E4031.<sup>28</sup>

Potassium channel activators rescued prolonged action potential of LQT2–hiPSC myocytes and in particular for the  $I_{kr}$  activator,

PD-118057, indicating that this class of drugs has a significant potential as an anti-arrhythmic agent against LQT2. Many compounds have been identified to increase  $I_{kr}$  currents through specific binding to different amino acid residues, and via several different mechanisms.<sup>36</sup> Such specificity could be tailored to patient treatment, depending on the mutation identified. In this scenario, patients could be administered with an appropriate  $I_{kr}$  channel activator to avoid using drugs that bind to protein sites at which amino acids had been substituted by mutation. Developing multiple hiPSCs lines, each with a unique genotype, would allow a degree of tailored drug evaluation to be carried out *in vitro* in functional cardiomyocytes carrying LQT2, which is an avenue we are investigating.

Administration of potassium channel openers in combination with isoprenaline was pro-arrhythmic, likely due to excessive shortening of the APD that elicited short-QT syndrome-like responses.<sup>11</sup> Therefore, it will be important to monitor the doses of potassium channel openers administered to patients. It may be possible to combine these drugs with  $\beta$ -blocker treatment,

which was shown here to attenuate EADs caused by acute shortening of the APD.  $\beta$ -Blockers have also been shown to attenuate nicorandil-induced tachycardia in canine *in vivo* models.<sup>37</sup> Combinatorial treatment could benefit cases where  $\beta$ -blocker treatment worsens bradycardia leading to a 23% increased incidence of cardiac events<sup>13</sup> or where arrhythmic events are caused during stimulation of the parasympathetic nervous system during sleep (22%).<sup>6</sup>

Overall, these data support the notion that hiPSC-derived cardiac myocytes can recapitulate the diseased phenotype of a heritable cardiac condition, and are consistent with recent reports of LQT1 and LQT2 (p.Ala614Val) hiPSC-based modelling.<sup>32,38</sup> However, there are important differences between our work with *KCNH2* G1681A (p.Ala561Thr) LQT2–hiPSCs when compared with the *KCNH2* p.Ala614Val mutation.<sup>38</sup> We identified isoprenaline as an inducer of APD shortening and EAD development, events not reported by Itzhaki *et al.*<sup>38</sup> and may relate to the mutation location in the ion channel. We have also shown that  $\beta$ -blockers used to manage cardiac electrophysiology in LQT2 patients elicit stabilizing effects in myocytes derived from LQT2–hiPSCs and that  $I_{Kr}$  channel activators, such as PD118057 represent a promising class of novel LQT2 anti-arrhythmic agents. Finally, we showed combined treatment with potassium channel enhancers and a  $\beta$ -adrenoreceptor stimulator led to excessive shortening of the APD, perturbing electrophysiology. This may indicate that potassium channel enhancers could be detrimental in patients experiencing stimulation of the sympathetic nervous system (e.g. exercise) and will require careful investigation before use.

In conclusion, we have developed a novel *in vitro* humanized system that will be useful for evaluation of new treatments for LQT2. Because the system relies on intact human cardiomyocytes that display a diverse expression profile of ion channels, it will complement the high throughput analysis employed using aneuploid cells (e.g. HEK293) transfected with a single channel gene. Indeed, a key challenge will be to improve the throughput of the hiPSC–cardiomyocyte system to allow a greater number of drugs to be tested at pharmaceutical levels. Once this is achieved, the human system will act as a comparator for myocytes isolated from animals, where species differences may confound interpretation. These activities will help rationalize datasets before drugs are tested in complex, organized three-dimensional *ex vivo* (heart slices, Langendorff system) or *in vivo* (intact animal or human hearts) models. Notably, the techniques presented here have the potential to influence future management and risk stratification of all forms of LQTS. They are also eminently translatable to many other conditions that affect the heart (acquired LQTS, cardiac failure or hypertrophy), as well as other heritable human disorders.

## Authors' contributions

E.M. was involved in production and analysis of hiPSC lines, derivation, and characterization of cardiomyocytes, electrophysiology; D.R. did electrophysiology data processing; E.D. was involved in optimization of hiPSC protocols; L.Y. established hiPSC capability;

I.M. was involved in electrophysiology; A.S. collected patient samples; C.D. is the project leader.

## Supplementary material

Supplementary material is available at *European Heart Journal* online.

## Acknowledgements

We thank Dr David Darling for BL15 cell line, Dr Nigel Smith for karyotype analysis, and Dr Mojgan Reza for advice in deriving skin fibroblast cells.

## Funding

Work was funded by British Heart Foundation, Medical Research Council, and Biotechnology and Biological Sciences Research Council. Funding to pay the Open Access publication charges for this article was provided by The University of Nottingham.

## References

- Morita H, Wu J, Zipes DP. The QT syndromes: long and short. *Lancet* 2008;**372**: 750–763.
- Hunt DP, Tang K. Long QT syndrome presenting as epileptic seizures in an adult. *Emerg Med J* 2005;**22**:600–601.
- Keller DL, Grenier J, Christe G, Dubouloz F, Osswald S, Brink M, Ficker E, Chahine M. Characterization of novel *KCNH2* mutations in type 2 long QT syndrome manifesting as seizures. *Can J Cardiol* 2009;**25**:455–462.
- Schwartz PJ. Idiopathic long QT syndrome: progress and questions. *Am Heart J* 1985;**109**:399–411.
- Bokil NJ, Baisden JM, Radford DJ, Summers KM. Molecular genetics of long QT syndrome. *Mol Genet Metab* 2011;**101**:1–8.
- Medeiros-Domingo A, Iturralde-Torres P, Ackerman MJ. [Clinical and genetic characteristics of long QT syndrome]. *Rev Esp Cardiol* 2007;**60**:739–752.
- Moss AJ, Zareba W, Kaufman ES, Gartner E, Peterson DR, Benhorin J, Towbin JA, Keating MT, Priori SG, Schwartz PJ, Vincent GM, Robinson JL, Andrews ML, Feng C, Hall WJ, Medina A, Zhang L, Wang Z. Increased risk of arrhythmic events in long-QT syndrome with mutations in the pore region of the human ether-a-go-go-related gene potassium channel. *Circulation* 2002;**105**: 794–799.
- Lehnart SE, Ackerman MJ, Benson DW Jr, Brugada R, Clancy CE, Donahue JK, George AL Jr., Grant AO, Groft SC, January CT, Lathrop DA, Lederer WJ, Makielski JC, Mohler PJ, Moss A, Nerbonne JM, Olson TM, Przywara DA, Towbin JA, Wang LH, Marks AR. Inherited arrhythmias: a National Heart, Lung, and Blood Institute and Office of Rare Diseases workshop consensus report about the diagnosis, phenotyping, molecular mechanisms, and therapeutic approaches for primary cardiomyopathies of gene mutations affecting ion channel function. *Circulation* 2007;**116**:2325–2345.
- Yang HT, Sun CF, Cui CC, Xue XL, Zhang AF, Li HB, Wang DQ, Shu J. HERG-F463L potassium channels linked to long QT syndrome reduce I(Kr) current by a trafficking-deficient mechanism. *Clin Exp Pharmacol Physiol* 2009;**36**: 822–827.
- Moss AJ, Zareba W, Hall WJ, Schwartz PJ, Crampton RS, Benhorin J, Vincent GM, Locati EH, Priori SG, Napolitano C, Medina A, Zhang L, Robinson JL, Timothy K, Towbin JA, Andrews ML. Effectiveness and limitations of beta-blocker therapy in congenital long-QT syndrome. *Circulation* 2000;**101**:616–623.
- Patel C, Antzelevitch C. Pharmacological approach to the treatment of long and short QT syndromes. *Pharmacol Ther* 2008;**118**:138–151.
- Priori SG, Schwartz PJ, Napolitano C, Bloise R, Ronchetti E, Grillo M, Vicentini A, Spazzolini C, Nastoli J, Bottelli G, Folli R, Cappelletti D. Risk stratification in the long-QT syndrome. *N Engl J Med* 2003;**348**:1866–1874.
- Priori SG, Napolitano C, Schwartz PJ, Grillo M, Bloise R, Ronchetti E, Moncalvo C, Tulipani C, Veia A, Bottelli G, Nastoli J. Association of long QT syndrome loci and cardiac events among patients treated with beta-blockers. *J Am Med Assoc* 2004;**292**:1341–1344.
- Zareba W, Moss AJ, Daubert JP, Hall WJ, Robinson JL, Andrews M. Implantable cardioverter defibrillator in high-risk long QT syndrome patients. *J Cardiovasc Electrophysiol* 2003;**14**:337–341.
- Sanguinetti MC, Tristani-Firouzi M. hERG potassium channels and cardiac arrhythmia. *Nature* 2006;**440**:463–469.

16. Ren X-Q, Liu G-X, Organ-Darling LE, Zheng R, Roder K, Jindal HK, Centracchio J, McDonald TV, Koren G. Pore mutants of HERG and KvLQT1 downregulate the reciprocal currents in stable cell lines. *Am J Physiol Heart Circ Physiol* 2010;**299**: H1525–1534.
17. Yu J, Vodyanik MA, Smuga-Otto K, Antosiewicz-Bourget J, Frane JL, Tian S, Nie J, Jonsdottir GA, Ruotti V, Stewart R, Slukvin II, Thomson JA. Induced pluripotent stem cell lines derived from human somatic cells. *Science (New York, NY)* 2007;**318**:1917–1920.
18. Dick E, Matsa E, Bispham J, Reza M, Guglieri M, Staniforth A, Watson S, Kumari R, Lochmuller H, Young L, Darling D, Denning C. Two new protocols to enhance the production and isolation of human induced pluripotent stem cell lines. *Stem Cell Res* 2011;**6**:158–167.
19. Anderson D, Self T, Mellor IR, Goh G, Hill SJ, Denning C. Transgenic enrichment of cardiomyocytes from human embryonic stem cells. *Mol Ther* 2007;**15**: 2027–2036.
20. Dausse E, Berthet M, Denjoy I, André-Fouet X, Cruaud C, Benceur M, Fauré S, Coumel P, Schwartz K, Guicheney P. A mutation in HERG associated with notched T waves in long QT syndrome. *J Mol Cell Cardiol* 1996;**28**:1609–1615.
21. Chugh SS, Senashova O, Watts A, Tran PT, Zhou Z, Gong Q, Titus JL, Hayflick SJ. Postmortem molecular screening in unexplained sudden death. *J Am Coll Cardiol* 2004;**43**:1625–1629.
22. Burridge PW, Anderson D, Priddle H, Barbadillo Munoz MD, Chamberlain S, Allegrucci C, Young LE, Denning C. Improved human embryonic stem cell embryoid body homogeneity and cardiomyocyte differentiation from a novel V-96 plate aggregation system highlights interline variability. *Stem cells (Dayton, Ohio)* 2007;**25**: 929–938.
23. Hoffman LM, Carpenter MK. Characterization and culture of human embryonic stem cells. *Nat Biotechnol* 2005;**23**:699–708.
24. Mummery C, Ward-van Oostwaard D, Doevendans P, Spijker R, van den Brink S, Hassink R, van der Heyden M, Opthof T, Pera M, de la Riviere AB, Passier R, Tertoolen L. Differentiation of human embryonic stem cells to cardiomyocytes: role of coculture with visceral endoderm-like cells. *Circulation* 2003;**107**: 2733–2740.
25. Schwartz PJ, Priori SG, Spazzolini C, Moss AJ, Vincent GM, Napolitano C, Denjoy I, Guicheney P, Breithardt G, Keating MT, Towbin JA, Beggs AH, Brink P, Wilde AAM, Toivonen L, Zareba W, Robinson JL, Timothy KW, Corfield V, Watanasirichaigoon D, Corbett C, Haverkamp W, Schulze-Bahr E, Lehmann MH, Schwartz K, Coumel P, Bloise R. Genotype–phenotype correlation in the long-QT syndrome : gene-specific triggers for life-threatening arrhythmias. *Circulation* 2001;**103**:89–95.
26. Clur SA, Chockalingam P, Filippini LH, Widyanti AP, Van Crujnsen M, Blom NA, Alders M, Hofman N, Wilde AA. The role of the epinephrine test in the diagnosis and management of children suspected of having congenital long QT syndrome. *Pediatr Cardiol* 2009;**31**:462–468.
27. Shimizu W, Tanabe Y, Aiba T, Inagaki M, Kurita T, Suyama K, Nagaya N, Taguchi A, Aihara N, Sunagawa K, Nakamura K, Ohe T, Towbin JA, Priori SG, Kamakura S. Differential effects of beta-blockade on dispersion of repolarization in the absence and presence of sympathetic stimulation between the LQT1 and LQT2 forms of congenital long QT syndrome. *J Am Coll Cardiol* 2002;**39**: 1984–1991.
28. Perry MD, Sanguinetti MC, Mitcheson JS. Revealing the structural basis of action of hERG potassium channel activators and blockers. *J Physiol* 2010;**588**: 3157–3167.
29. Jentsch TJ, Hubner CA, Fuhrmann JC. Ion channels: function unravelled by dysfunction. *Nat Cell Biol* 2004;**6**:1039–1047.
30. Biermann J, Wu K, Odening KE, Asbach S, Koren G, Peng X, Zehender M, Bode C, Brunner M. Nicorandil normalizes prolonged repolarisation in the first transgenic rabbit model with long-QT syndrome 1 both *in vitro* and *in vivo*. *Eur J Pharmacol* 2010;**650**:309–316.
31. Kong CW, Akar FG, Li RA. Translational potential of human embryonic and induced pluripotent stem cells for myocardial repair: Insights from experimental models. *Thromb Haemost* 2010;**104**:30–38.
32. Moretti A, Bellin M, Welling A, Jung CB, Lam JT, Bott-Flugel L, Dorn T, Goedel A, Hohnke C, Hofmann F, Seyfarth M, Sinnecker D, Schomig A, Laugwitz KL. Patient-specific induced pluripotent stem-cell models for long-QT syndrome. *N Engl J Med* 2010;**363**:1397–1409.
33. Wood AJJ, Roden DM. Drug-induced prolongation of the QT interval. *N Eng J Med* 2004;**350**:1013–1022.
34. Peng S, Lacerda AE, Kirsch GE, Brown AM, Bruening-Wright A. The action potential and comparative pharmacology of stem cell-derived human cardiomyocytes. *J Pharmacol Toxicol Methods* 2010;**61**:277–286.
35. Shimizu W, Antzelevitch C. Effects of a K(+) channel opener to reduce transmural dispersion of repolarization and prevent torsade de pointes in LQT1, LQT2, and LQT3 models of the long-QT syndrome. *Circulation* 2000;**102**: 706–712.
36. Grunnet M, Hansen RS, Olesen SP. hERG1 channel activators: a new anti-arrhythmic principle. *Prog Biophys Mol Biol* 2008;**98**:347–362.
37. Humphrey SJ. Cardiovascular and pharmacokinetic interactions between nicorandil and adjunctive propranolol, atenolol or diltiazem in conscious dogs. *Methods Find Exp Clin Pharmacol* 1998;**20**:779–791.
38. Itzhaki I, Maizels L, Huber I, Zwi-Dantsis L, Caspi O, Winterstern A, Feldman O, Gepstein A, Arbel G, Hammerman H, Boulos M, Gepstein L. Modelling the long QT syndrome with induced pluripotent stem cells. *Nature*; doi:10.1038/nature09747. Published online ahead of print 16 January 2011.